International Journal of Thin Films Science and Technology

http://dx.doi.org/10.18576/ijtfst/130209

Study of the Dynamic Properties of Chaotic Circuits in the Presence of Memristors

Zainab S. Kareem[1] *and Hussein B. Al Husseini*[1, 2, *]

[1] Department of Physics, College of Sciences, University of Thi-Qar, Thi-Qar, Iraq
[2] College of Education, Al-Ayen Iraqi University, Thi-Qar, 64001, Iraq

Received: 18 Feb. 2024, Revised: 23 Apr. 2024, Accepted: 27 Apr. 2024
Published online: 1 May 2024

Abstract: In this paper, the inaugural subject covered is a memristor model with three distinct circuits that is based on a multi-segment linear function. The dynamic behavior of these circuits is then examined in terms of bifurcations, coexisting attractors, and complexity based on various values of the inserted memristor parameters. Several dynamic features of these circuits, such as period-doubling bifurcations, chaotic bursts, and chaotic transients, are revealed via bifurcation analysis. Muthuswamy displays dynamic phenomena with varying beginning circumstances, such as coexisting attractors, multi-stability, and super multi-stability. Furthermore, circuit simulation was employed to confirm the Chua circuit's existence and viability. The purpose of coexistence circuits is to produce attractors capable of altering any state variable's initial value. The benefits of the suggested system, such as controlled attractor number and direction, an easy-to-implement circuit, and rich dynamic behavior, are demonstrated by comparison with other chaotic attractors. Finally, the coexistence of several chaotic attractors and the replacement of the exponential formula with a memristor formula increase the stability of the Colpitts circuit. Simulation results show that the three circuit schemes proposed in this article require less time to achieve full dynamics than other circuit schemes. This feature improves the effectiveness and usability of the proposed circuit strategy in practical applications.

Keywords: memristor, Muthuswamy, Chua, Colpitts, chaotic attractors.

1 Introduction

Professor Leon Chua discovered memristors at the University of California, Berkeley in 1971. It is thought that memristors are the fourth missing passive circuit element. Transistors and operational amplifiers were employed by him to construct this memristor. All currents and voltages have a dynamic range, and the operating frequency is determined by transistors and amplifiers. In spite of the fact that memristors are passive devices—the laboratory model has an internal power supply—Chua's memristor is active [1].

Through a thin coating of titanium dioxide, a team at Hewlett-Packard Labs (HP Labs) announced the development of the memristor on May 1, 2008, in the journal Science [2], after nearly 38 years of scientific endeavor. Apart from resistors, capacitors, and inductors, memristors are also available. They are similar to resistors in many ways, including the use of the ohm measurement unit. The resistance of this novel gadget when the power is switched off has received a lot of attention; to put it another way, it depends on the integral of the whole previous current waveform. As a result, memristors are nonlinear and have numerous special characteristics [3].

This has led to its application in many different fields, such as electrical engineering and computer science. They've seen widespread application in both hardware security and neural networks [4-5]. Wang and colleagues [6] developed a chaotic mnemonic technique to accomplish image encryption. It was demonstrated by Tan and Wang [7] that a neural model of two memristor-based neurons exhibits discrete firing pattern transitions and attractors. Memory can also be used to generate digital signals [8] and programmable circuitry [9]. Much work has been done on the analysis of the dynamic behavior of circuits with memories [10]. It has been shown that memristors, together with resistors, capacitors, and inductors, are the main component of simple electrical circuits [11].

The structure of this document is as follows. The memristor, the mathematical model, and a few parameter values that are often used in the literature are introduced in Section 2. Section 3 presents three circuit elements in series, Muthuswamy circuit is the simplest circuit, a modified Colpitts circuit, and a modified Chua memristor circuit. As explained in Subsection 3.1, the three circuit elements connected in series can display both chaotic and hyper-chaotic attractors, depending on the parameter values. Coexisting attractors are present in modified memristor circuits based on Chua and Colpitts oscillators, as demonstrated in subsections 3.2 and 3.3. In Section 4, finally is our conclusion.

*Corresponding author E-mail: drhussain@sci.utq.edu.iq

2 Memristor

A memristor is an electrical circuit device with two terminals that has a variable resistance [12] in response to the total amount of charge flowing through it [13]. Chua showed that circuits built with simply the resistor (R), capacitor (C), and inductor (L)—the other three essential electrical components—could not mimic the behavior of a memristor, proving that the memristor is indeed fundamental.

Chua gave a mathematical explanation of how his imaginary gadget would result in a flux and charge relationship that is similar to the voltage and current relationship that a nonlinear resistor produces. There was no obvious physical connection between charge and the integral over voltage prior to HP's discovery. Stanley Williams explained how the discovery of the missing memristor connected to the Chua mathematical model [1].

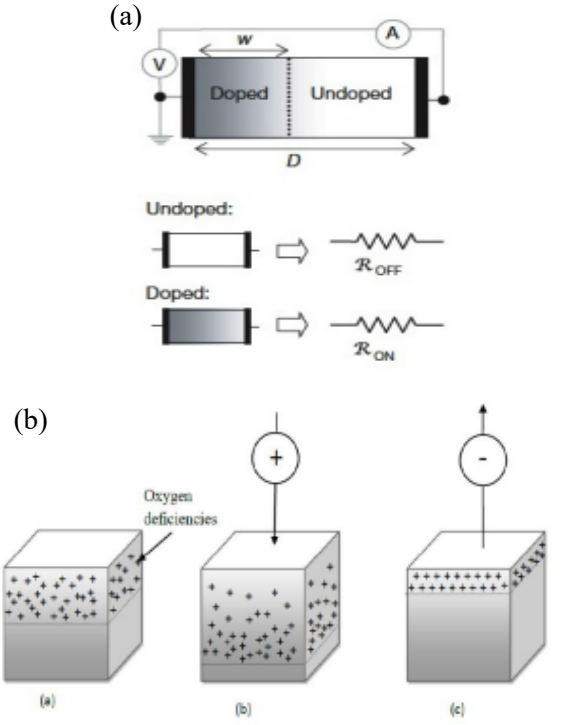

Fig. 1: TiO_2 Memristor (a) Schematic of TiO_2 Memristor (b) TiO_2 Memristor's behavior when applied to both positive and negative voltages [1] .

Fig. (1) illustrates the distribution of oxygen vacancy bubbles in the upper layer of TiO_{2-x}, which suggests oxygen deficiencies [1]. A positive bias on the switch drives the (positive) oxygen deficits to fall into the insulating TiO_2 layer below by rejecting them in the metallic top TiO_{2-x} layer. The boundary between the two materials moves downward and the fraction of conducting TiO_{2-x} rises, increasing the conductivity of the entire switch. A higher positive voltage causes the cube to become more conductive. The positively charged oxygen bubbles are drawn out of the TiO_2 by the switch's negative voltage. As the amount of resistive insulating TiO_2 increases, the switch becomes resistive overall. The more negative voltage applied, the less conductive the cube gets. This switch is special because the oxygen bubbles inside it remain stationary when the voltage, either positive or negative, is turned off. The two layers of titanium dioxide are frozen at their border because they never move. In this manner, the Memristor "remembers" how much voltage was applied at that time.

The word "memory resistor" is sometimes shortened to "memristor" as remembering one's state history accurately is a memristor's primary function. The memristor is an excellent option for storing nonvolatile memories for the following generation due to its important characteristic. By combining with transistors without reducing transistor size, memristors can significantly improve digital chip performance in hybrid circuits. It has little power consumption, limited scalability, and a variable charge or flux.

The memristor was first defined by a non-linear functional connection between the magnetic flux linkage, Φ(t), and the amount of electric charge that had flowed. According to symmetry considerations [15], a fourth fundamental circuit element for determining a φ–q relationship makes sense, as shown by Fig. (2).

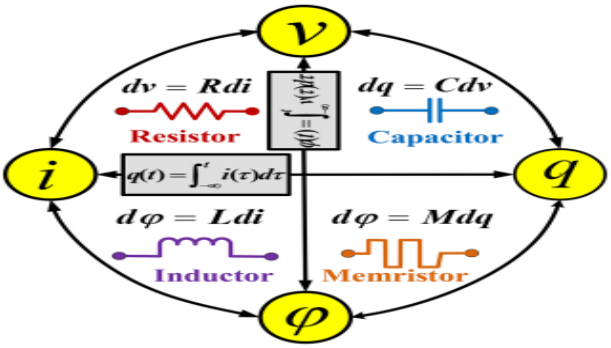

Fig. 2: The four fundamental two-terminal circuit elements and the matching reference directions are related to the fundamental circuit variables by virtue of the elements' rules. [39].

The fundamental circuit variables are connected to the relevant reference directions. The components are the capacitor, memristor, resistor, and inductor, arranged counterclockwise from top left. Remember that the speed at which charges flow is called current. Voltage has two meanings that are incompatible with each other according to electromagnetic field theory. Nonlinear circuit elements use the same symbols as basic circuit elements.

As a result, a memristor is any dynamical electronic circuit element that satisfies the Chua memristor equations [16]. Regardless of the underlying physics of the system that gives birth to the relations:

$$V = R(\omega,q).i \quad or \quad V = M(\omega,q).i \tag{1}$$

where ω is the device's state variable, i is the electric current, R or M (ω, q) is the generalized resistance, and V is the voltage potential [17]. Memoristance defines a linear relationship between current and voltage, as this equation demonstrates, provided that charge stays constant. Of course, a current that is not zero denotes an instantaneous charge. Nevertheless, by providing a measurable voltage without net charge movement, changing current may show the linear dependency in circuit operation if the greatest change in q does not result in a significant change in M (ω, q).

$$M = R_{ON}\frac{\omega}{D} + R_{OFF}(1-\frac{\omega}{D}) \tag{2}$$

RON and ROFF, respectively, High resistance in low concentration dopant and Low resistance in high concentration dopant in [18]. D is the overall length of the memristor. Since (G = 1/M) represents the memductance, Eq. (1) can be recast as (i = G· V). Where t is the time, η is the polarity, and v_o is the voltage amplitude, and T is the potential oscillation period. According to equation (3), f (ω, p) = 1 − (2ω − 1) 2p. the nonlinear dopant drift's window function, where p is a positive integer.

Table 1: Description and values of parameters [20]

Description	Parameter	Value
η	**Polarity**	**1**
D	**Length of titanium diode memristor**	**1 nm**
R_{OFF}	**High resistance in low concentration dopant**	**70 Ω**
R_{ON}	**Low resistance in high concentration dopant**	**1 Ω**
P	**Integer value in the nonlinear function**	**10**
v_0	**Voltage Amplitude**	**1 V**
T	**Intrinsic period of oscillation**	**20 s**
ω_o	**Initial device value**	**e [0.0,1.0] nm**

Table (1) [19] shows the description and some values of the parameters that are frequently used in the literature. We demonstrate the typical temporal behavior of a memristor by applying a periodic voltage V (t) to it.

$$\omega^{g} = \eta.\mathrm{f}(\omega,\mathrm{p}).i = \frac{\eta.\mathrm{f}(\omega,\mathrm{p}).\mathrm{V}}{M}$$

$$V = v_o.\sin(\frac{2\pi t}{T})$$

$$\omega^{g} = \frac{\eta.\mathrm{f}(\omega,\mathrm{p})v_o.\sin(\frac{2\pi t}{T})}{R_{ON}\frac{\omega}{D} + R_{OFF}(1-\frac{\omega}{D})} \tag{3}$$

Where Eq .(1) is the quasi-static resistance equation, also known as state-dependent Ohm's law, and equation (3) is the dynamical equation that shows the temporal evolution of the state variable (or variables) ω as a function f(ω,p) of ω and possibly the current (or alternatively voltage if one is considering the conductance of the element). In these equations, ω o is an independent input function and often a function of time. The resistance R, which depends on the physical state ω, which provides the device memory, and perhaps the current i, yields a nonlinear Ohm's law. Even though they are both constructed of materials called transition metal oxides, the approach to simulating nonlinear devices is virtually quite effective.

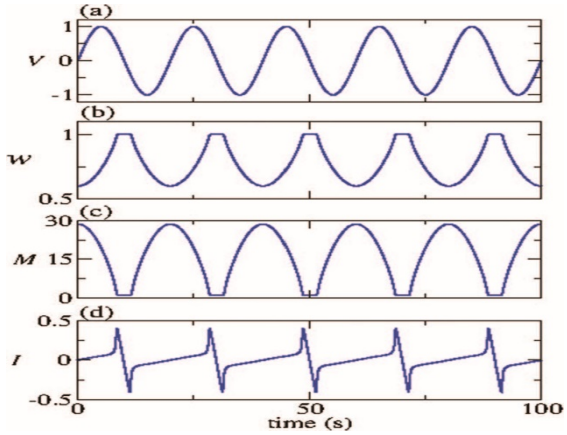

Fig. 3: Time series of (a) V , (b) ω, (c) M, and (d) I We consider the parameters according to Table (1. 2)We observe periodic oscillations [20].

Consequently, current flowing behind set I and the memresistance variable M are shown in Fig. (3). The device's state variable has an initial resistance of M(ω_o) as maximal and an initial value of $\omega_{(t=0)} = \omega_o$ as minimal. We can observe that the memristor device's state (Fig. 3(b)) can be altered by oscillation in the applied voltage (Fig. 3(a)). The current flowing through the device Fig. (3(d)) oscillates as a result of the memresistance Fig. (3(c)).

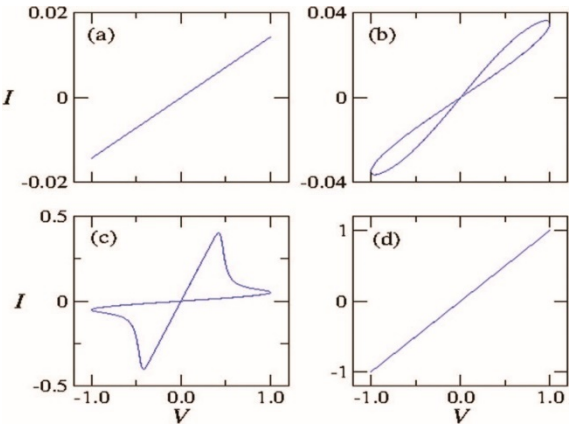

Fig. 4: I for (a) ω_o = 0 nm, (b) ω_o = 0.5 nm, (c) ω_o = 0.6 nm, and (d) ω_o = 0.8 nm as a function of V. One can see that a pinched hysteresis effect exists depending on ω_o, as illustrated in panels (b) and (c) [20].

Fig. (4) shows i as a function of V for different values of ω_o. Fig. (4) (a) shows that for ω_o = 0.0 nm, i is directly proportional to V. In Fig. 4(b) and (c), we see a for ω_o = 0.5 nm and 0.8 nm, respectively.

The current-voltage characteristic of the memristor device is called the pinched hysteresis effect. At ω_o = 0.8 nm, the i - V curve makes a straight pass across the origin. The i×V curves can be obtained by considering V = $v_o \cdot \sin(2\pi t/t)$ [20].

3 Behavior of chaos circuits in the presence of a memristor

We employ three chaotic circuits to add the second-order (M(ω,q)= W(ω,q))-formula memristor to the Muthuswamy-Chua, Chua, and Colpitts circuits, and the resulting behavior is as follows [21] :

3.1 Muthuswamy- chua circuit

It was suggested to use the most basic electronic circuit to create chaotic attractors. The appropriate block diagram is shown in Fig. (5). It is made up of a linear passive inductor, a linear passive capacitor, and a nonlinear [22] active memristor. This electronic circuit can be described by these three differential equations [15, 23, 24].

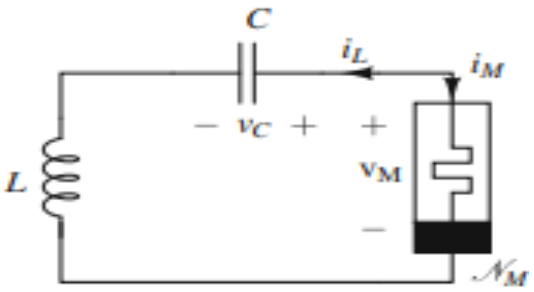

Fig. 5: The circuit known as Muthuswamy-Chua [20].

Fig. (5) depicts the most basic chaotic circuit [25]. The equation system is independent because it takes three state variables to cause chaos in a self-contained continuous-time system. A memristor-based circuit with just three parts was proposed by Muthuswami and Chua: a linear negative inductor; a nonlinear active memristor with a second-order polynomial memory W(r). with a negative linear capacitor. The memristor would then be able to have its own separate 3-Dimensional Ordinary Differential Equations model.

$$V_M = \beta(x^2 - 1) i_M$$
$$W(r = x) = \beta(r^2 - 1)$$
$$\frac{dr}{dt} = i_M - \alpha x - i_M \quad (4)$$

V_M represents the voltage across the ends of the memristor, i_M represents the current flowing through it, and r is an interal variable in this memristive model [26]. The mathematical description of Fig. (5) can be achieved by applying KV and KC law to electrical circuits .

$$C \frac{dV_C}{dt} = i_L$$
$$L \frac{di_L}{dt} = W(r) i_M - V_C$$
$$\frac{dx}{dt} = i_M - \alpha x - i_M \quad (5)$$

Muthuswamy equations with memristor [24] is the mathematical model that explains the behavior of the circuit.

$$x^{\cdot} = \alpha y$$
$$y^{\cdot} = -b(W(z) y + x)$$
$$z^{\cdot} = -y - \alpha z + y z \quad (6)$$

(x = V_C) where the voltages across the capacitor, (i_L = y) the current through the inductor, (r = z) the voltages in memristor, (a = 1/C), (b = 1/L) represent fixed parameters and are included in the Eq . (6).

Examining the relationship between the capacitor's voltage and the control parameter α, which creates the bifurcation diagram, allows one to see the chaotic dynamics of continuous parameter change.

In addition to any changes in its parameters, a time series was generated, resulting in a bifurcation diagram. If we substitute the values a = 0 .83, b = 0 .3, and β = 1.34 [20] into the Muthusamy -Chua circuit equations, we can observe the shape of Fig. (6) as a function of the control parameter α.

The effect of α with voltages across the capacitor is discussed in Fig. (6) as an earlier works [20]. The drawing makes clear that the circuit exhibits rich dynamic behavior, beginning with periodic, moving through chaotic regions interspersed with the coexistence of various patterns, and ending at value 1 when α, which causes the double periodicity's basic behavior to repeat, followed by periodicity.

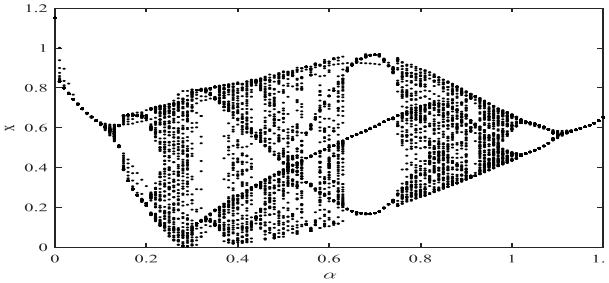

Fig. 6: The relationship between the voltage in the capacitor and the control parameter α.

Increasing the value of b in Fig. (7) will show that at b = 0.43 we obtain a bifurcation diagram that generally resembles Fig. (6) but with a different periodic amplitude; It initially reaches 2.5, then decreases until it reaches 1, and becomes periodic, while from 0.1 to 0.8 it is a chaotic region with high dynamics. Finally, we notice that it becomes quasi-periodic from α = 0.8 to the end in Fig. (7(a)).

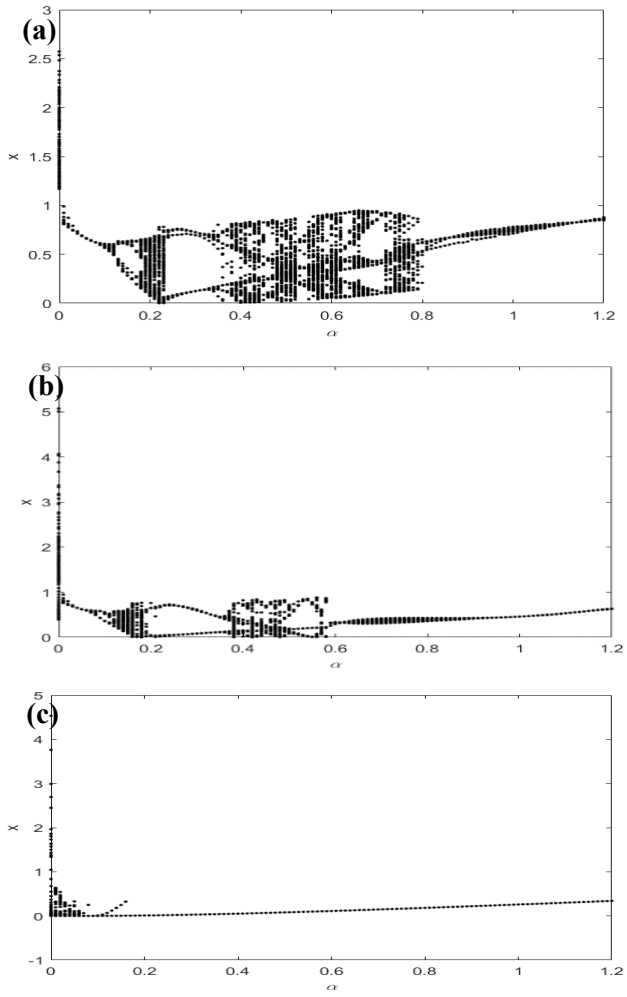

Fig. 7: The relationship between the voltage in the capacitor and the control parameter α (a) L=2.3 (b) L=1.2 (c) L=0.3.

When b = 0.8 in Fig. (7 (b)), the amount of the chaotic attractor dropped dramatically from Fig. (7 (a)), as the single-periodic became less than before and the amplitude of periodicity grew larger than 5. After a brief period of unrest. Subsequent to the 0.2 to 0.4 periodic binary areas, we observe that the chaos zone shrank, causing the periodic region to expand from 0.6 to 1.2 in size.

The bi periodic component was relatively tiny, and the region close to the voltage axis became chaotic with a capacitance higher than 4. When b = 3.3 in Figure (7(c)), we may state that the amount of chaotic attractor drastically reduced or nearly vanished from its previous value. It used to be tiny and resulted in a greater periodicity between 0.2 and 1.2.

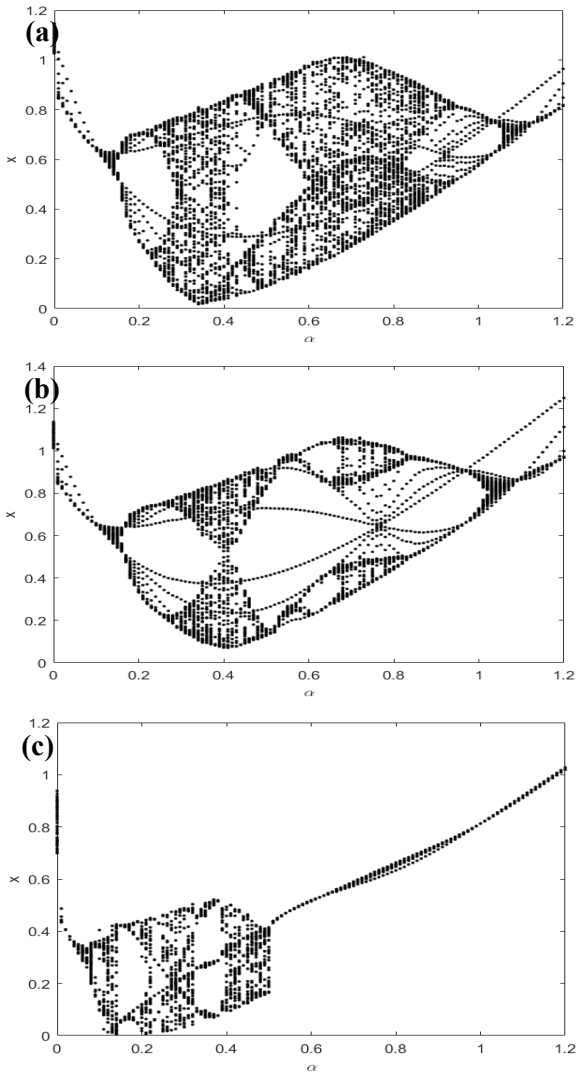

Fig. 8: The relationship between the voltage in the capacitor and the control parameter α (a) C=1.2, L=4.3 (b) C=1.2,L=5.3 (c) C=2.2, L=5.3.

As we decrease the value of b = 0.23, we see that Fig. (8 a) shows a semi-periodic zone, followed by a region of chaos with dynamics interleaved between 0.2 and 1, disorderly contraction to form a little periodic area and, at the end, a doubly periodic zone.

In Fig. (8(b)) has resemblance to Figure (8(a)) at b = 0.188. A high degree of dynamism is intermingled with a fraction of chaotic gravity thereafter. The periodic pentagons, hexagons, and tetrads are likewise restricted to the range of 0.2 to 1. We next locate the quasi-trigonal region, which has a periodicity between 1 and 1.2.

As for Fig. (8(c)), we discover that the chaotic zone becomes restricted between 0.1 and 0.5, where it acts almost the same when it becomes (b=3.3), while the periodic region almost exists if we increase the amplitude

(a = 0.45) and (b = 0.188). however, by raising (a). The range of 0.5 to 1.2 is then found to be quasi-periodic.

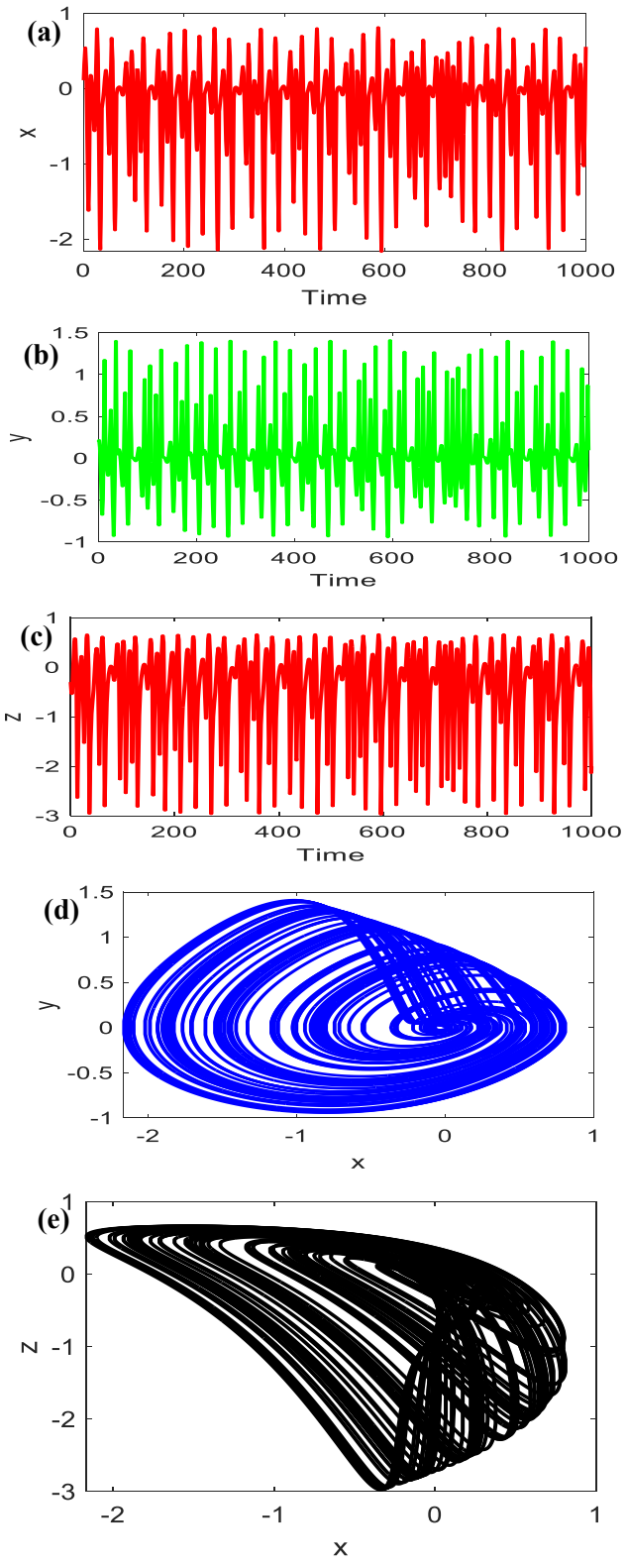

Fig. 9: Time series for (b=0.3 , α=0.4) and The chaotic attractor of charge-controlled memristor based on the simplest chaotic circuit.

Taking the time series and chaotic attraction plots for charge control in Fig. (9), we observe that when b = 0.3, a = 0.83, and β = 1.34, and when we take α = 0.4, we observe that in Fig. (9). a) We note that the plot is in a state of chaos and non-repetition, that is, a quasi-explosion was found non-periodicly and with different amplitudes, as in Fig. ((9 (b and c)))

Using the simplest chaotic circuit as a basis, Eq. (6) may be used to calculate the time series of (b=0.3, α=0.4) and the chaotic attractor of the charge-controlled memristor (a) Chaotic path ($i_L(t)$ vs V_C; (b) Chaotic route (r versus V_C). It is seen that the right portion of the image exhibits an overwhelming chaotic attraction, whilst the left side displays a periodic condition with a near amplitude in Fig. (9).

According to our observations, increasing the parameter (b) reduces the chaos, where b is the inverse of the inductance. However, when we reduce the value of (b) as well as the value of (a), we find that it may behave similarly when (b) is large. This is because a represents the reciprocal of the capacitor, which means that as b increases, L decreases, and the resulting chaos across the voltages in the capacitor decreases. When we increase L and decrease (b) , we find that the chaotic attraction in the voltages across the capacitor increases, and the opposite happens when we decrease L and increase (b), due to the properties of the conduction of the inductor and the capacitor, respectively, which reduces the resulting disturbance in the voltages across the capacitor.

3.2 Chua circuit

In 1983, the Chua circuit was created in an attempt to address two inquiries pertaining to the Lorenz equations that numerous academics had raised. This system was developed in order to demonstrate that chaos is a strong physical phenomenon and that efforts are made in order to formulate it realistically in the laboratory using the Lorenz equations. Another is to demonstrate using rigorous mathematical methods that the Lorenz attractor, discovered by computer modeling, really exists in a chaotic form.

The fundamental components of the Chua circuit are two capacitors, a resistor, an inductor, and a Chua diode. Here, in Fig.(8), we swap out the Chua diode for a memristor. In order to alter Chua's circuit, we added a nonideal voltage-controlled memristor with a quadratic internal state [32], which is described as follows:

$$i_M = W(r)\,V$$

$$W(r) = \alpha - \beta r^2$$

$$\frac{dr}{dt} = -cV_1 - d\,r_0 + V_1^2 r \tag{7}$$

where c,d,α,β are the system parameters and W(r) is the memristance, and r is the memristor's internal voltage. The

MCC's parameter values. The improved Chua's circuit with four nonlinear elements is depicted in Fig. (10).

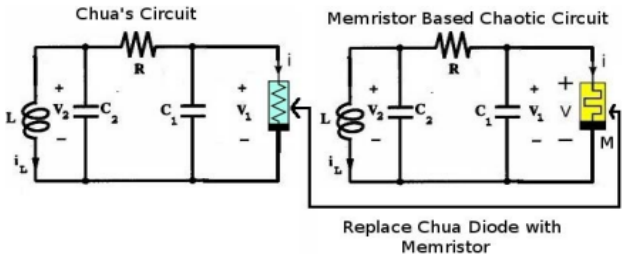

Fig. 10: The memristor chua circuit [3].

Kirchhoff's circuit laws are used to analyze the circuit and provide the following equation [33]:

$$C_1\frac{dV_1}{dt} = G(V_2 - V_1) - GW(r)V_1$$
$$C_2\frac{dV_2}{dt} = G(V_1 - V_2) - i_L$$
$$L\frac{di_L}{dt} = V_2$$
$$\frac{dr}{dt} = -cV_1 - d\,r + V_1^2\,r \tag{8}$$

Chua's dimensionless equations for analytical treatment, Eq. (8) are typically reformulated in a more practical form where... Starting with the circuit's state equations, we will quickly deduce these equations. By using $x = V_1,\ y = V_2,\ z = \frac{i_L}{G},\ t = \frac{C_2\tau}{G},\ \alpha = \frac{C_2}{C_1},\ b = \frac{C_2}{G^2L}$ and r = ω the rescaling the following is what happens to Eq. (8) when the values are changed [20]:

$$x^{\cdot} = a(y - x + W(\omega)x)$$
$$y^{\cdot} = x - y - z$$
$$z^{\cdot} = b\,y$$
$$\omega^{\cdot} = -c\,x - d\,\omega + x^2\,\omega \tag{9}$$

Where ω represents the internal voltage of the memristor, x and y correspond to the voltages in the capacitors C1 and C2, respectively, and z represents the current passing through the inductor iL. Memresistance W(ω) is determined by the following parameters: α, β, b, c, d, and eq. (17) [23].

To investigate the properties of the chua circuit after replacing the chua diode with a memristor, solve Eq. (9) using the Steady State system with coefficients α = 1.2, a = 14, b = 1.4, c = 37, and d = 12. The beta coefficient in bifurcated form with respect to the voltage across the first capacitor. We can see that in the event of a double-periodic phase, there is a positive and negative voltage across the first capacitor in Fig.(11).

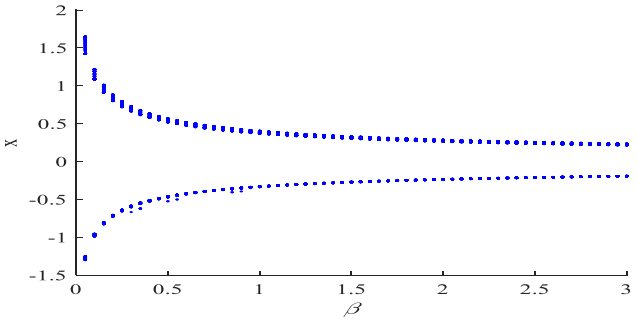

Fig. 11: The relationship between the voltage in the capacitor and the control parameter β.

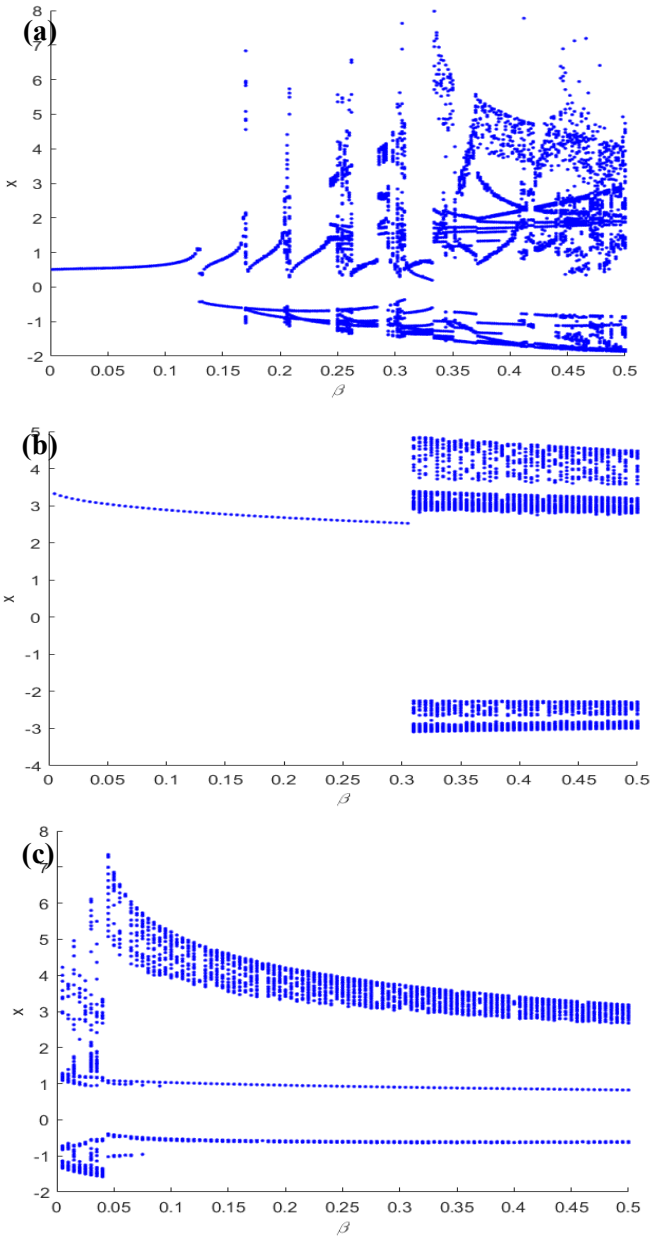

Fig. 12: The relationship between the voltage in the capacitor and the control parameter β (a),d=0.1(b)d=0.5 (c)d=1.5.

In Fig. (12), for α = 1.2, a = 14, b = 0.2, and c = 1.8, we obtain a bifurcation diagram when analyzing the relationship between the voltage in the capacitor and the control parameter β. Changing d results in a shift in the bifurcation formula in Fig. (11), where two zones of chaos occur at 0.125, one at the positive voltage across the first capacitor and the other at the negative voltage, as illustrated in Fig. 12(a) at the beginning of the periodicity.

When the values of (d = 0.5) vary in Fig. (12(b)), we notice that the periodic component grows to 0.3, which is larger than it was in Fig. (12(a)). Then, it is divided into two components: the quasi-periodic part of the chaotic, which is negative, and the quasi-periodic part of the chaotic, which is positive. When combined, these components form a chaotic quasi-tripartite.

Figure 12(c) Once we adjust the value of (d = 1.5), we observe that it began chaotically and eventually settled to a value of roughly 0.5. The chaotic region was then split into two positive and one negative parts, forming a quasi-periodic triangle, with one of the positive parts appearing semi-chaotic.

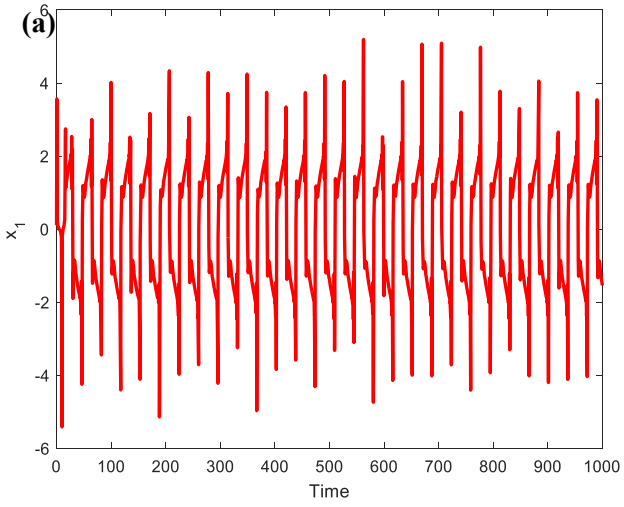

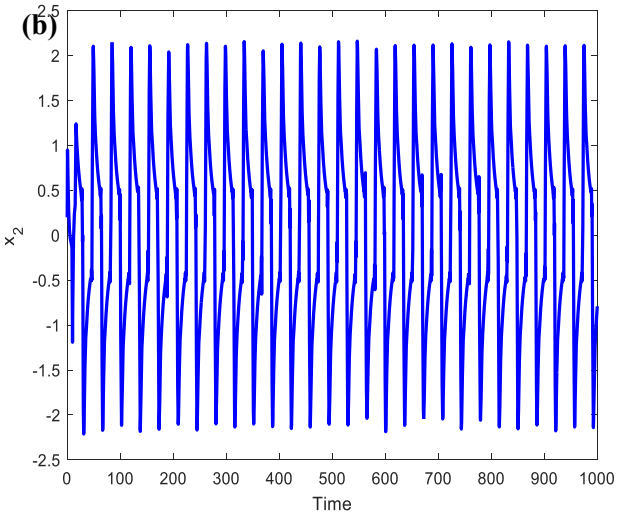

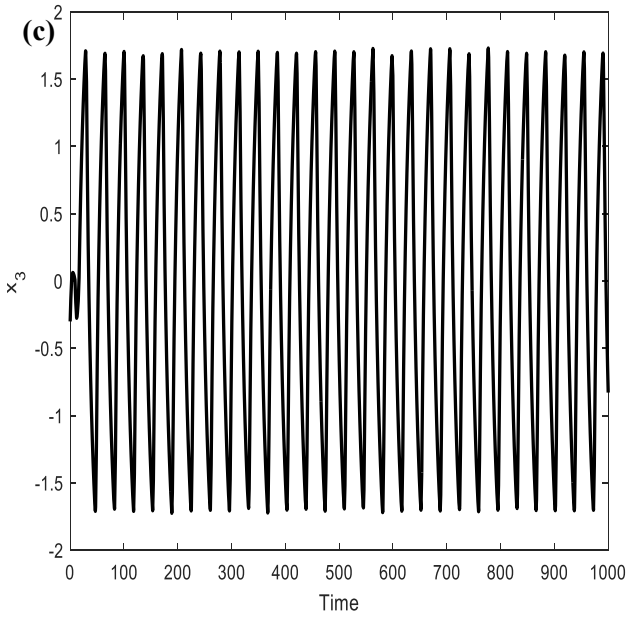

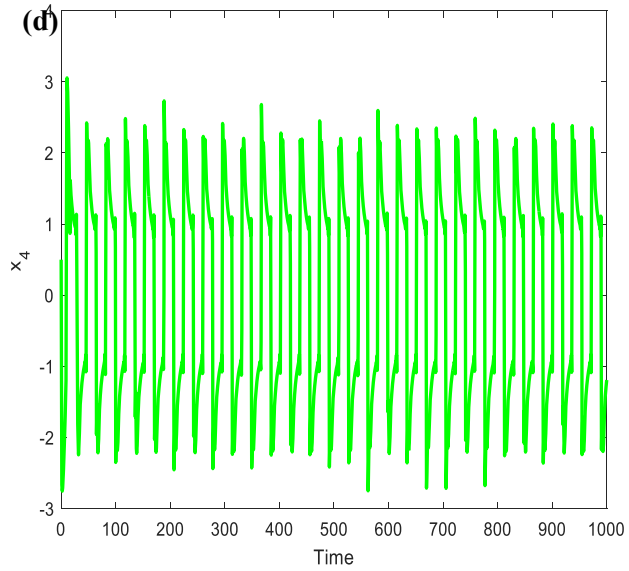

Fig. 13: Time series Fig .(12 (a)) when β=0.5.

Fig. (13) shows that the time series is when (α= 1.2, β=0.5, a=14,b=0.2,c=1.8,d=0.1) is as if it explains the bifurcation Fig. (12 (c)) when the voltage passes through the first capacitor (x1) and the voltages through the second capacitor (x2) or the current through the inductor (x3) and finally the voltages through the memristor (x4). Through that, we notice that Fig.(13 (a) describes the quasi-periodic voltage across the first capacitor, while (13 (b) is for a voltage across the second capacitor, which is more periodic than in the first capacitor, and at Fig.(13 (c)) we notice that it is a current through the inductor and we find it in a state of periodicity despite its turbulent beginning. The voltages across the memristor in Fig. 13(d) are described as being the same as in Fig. (13(a)) that is, they exhibit quasi-periodicity and instability in both Figs.

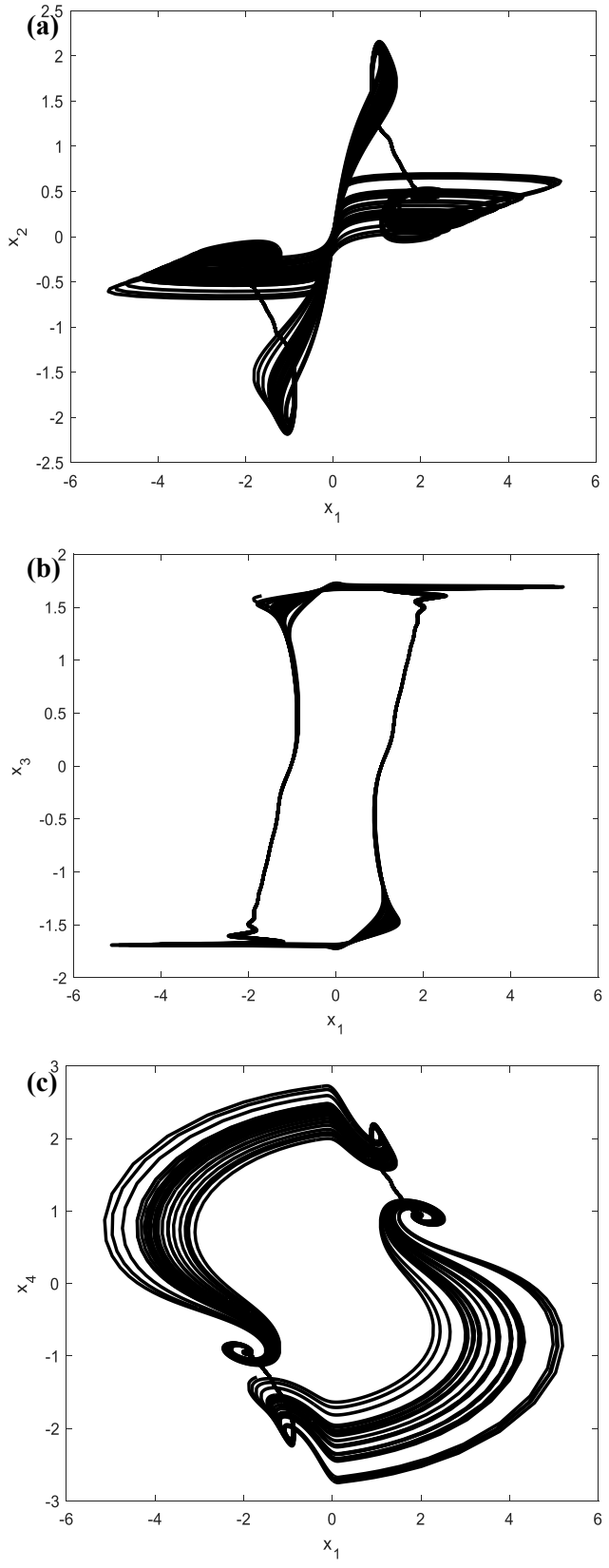

Fig. 14: New hyperchaotic attractor in voltage in the first capacitor (x_1) with (a) voltage in the second capacitor (x_2) (b) current across the inductor.

Fig. (14) shows the chaotic hyper-attractor of the voltage within the first capacitor when the values are α= 1.2, β=0.5, a=14, b=0.2, c=1.8, and d=0.1. in Fig. (14(a)) shows the voltage in the second capacitor, Fig. (14(b)) the current through the inductor, and Fig. (14(c)) the voltages in the memristor. This turns out to be a new kind of two-way symmetric periodic excessive chaos attractor.

According to our observations in the Chua circuit, the chaos reduces as factor (d) rises in the bifurcation form between the factor β and the voltage in the first capacitor when the diode is swapped out for a memristor. This causes the circuit to become linear, and when this factor drops, the opposite occurs. When nonlinear traits emerge, chaos is drawn to sameness and repetition.

3.3 Colpitts circuit

A resonant tank circuit, which establishes the oscillation frequency, is created by Colpitts [20] in 1918 using an inductor and two capacitors connected in parallel and bipolar junction transistor (BJT) . The oscillation frequency has a microwave range of a few Hz to 109 Hz. The periodic and chaotic behavior of this circuit is supported by experimental and numerical data [24, 25]. The Colpitts oscillator is very commonly utilized in communications systems and electronic gadgets. The circuit configuration is shown in Fig. (15).

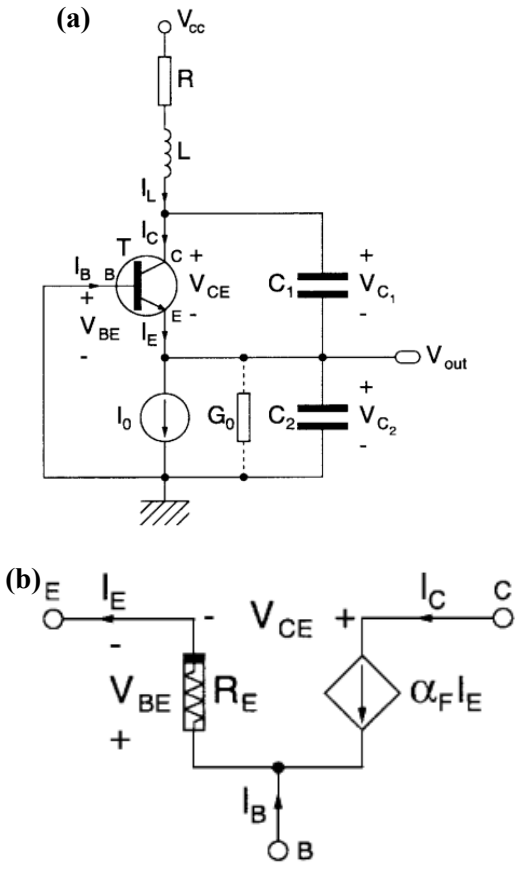

Fig. 15: (a)Colpitts Oscillator Circuit (b)Transistor (BJT)

[4].

Chaotic multicoil attractors derived from a modified Colpitts oscillator model Following the removal of the electrical source (V_{CC}), f (V_2) = $n(y) = e^{-y} - 1$ and io = 0, Eq.(10) takes on the following form:

$$\begin{aligned} C_1\frac{dV_1}{dt} &= i_L - f(v_2) & C_1\frac{dV_1}{dt} &= i_L - n(y) \\ C_2\frac{dV_2}{dt} &= i_L - i_O \quad\Rightarrow & C_2\frac{dV_2}{dt} &= i_L \\ L\frac{di_L}{dt} &= V_{CC} - V_1 - V_2 - Ri_L & L\frac{di_L}{dt} &= -V_1 - V_2 - Ri_L \end{aligned} \tag{10}$$

Using the dimensionless Colpitts Eq. (10), when we obtain the order dimension when adding the memristor formula instead of the exponential formula, which is n (y), the Eq.(10) becomes:

$$\begin{aligned} x^{\cdot} &= \frac{g}{Q(1-K)}\left(z - n(y)\right) & x^{\cdot} &= az - aW(\omega)y \\ y^{\cdot} &= \frac{g}{QK}z \quad\Rightarrow & y^{\cdot} &= az \\ z^{\cdot} &= \frac{QK(1-K)}{g}(x+y) - \frac{1}{Q}z & z^{\cdot} &= -0.5\frac{(x+y)}{a} - bz \\ & & \omega^{\cdot} &= y \end{aligned} \tag{11}$$

x and y stand for the voltages across the capacitors, and z is the current flowing through the inductor. In this context, the constants g, Q, and k are also implicated [27, 28]. For the sake of simplicity, a = 2g/Q and b = 1/Q are introduced [38].

If i_M is the current through the memristor and W(r) is the Memoristance, then the quadratic formula is ω = r representing the voltages across the memristor, where the memristor equation is:

$$\begin{aligned} W(\omega) &= \alpha - \beta\,\omega^2 \\ i_M &= W(r)\,V_2 \\ \frac{dr}{dt} &= V_2 \end{aligned} \tag{12}$$

The circuit properties are studied after the memristor formula was used in place of the exponential formula. This is done by utilizing the relationship between the voltages in the first capacitor and the control parameter α, as well as the values of β = 0.1, a = 5.2, and b = 0.9 for α. The results show that the circuit first exhibits stable behavior in Fig. (16(a)), but as α approaches 0.15, we notice that its amplitude has increased while maintaining periodicity. After that, it becomes a periodic quasi-double, returning to a periodic quasi-double for a short while. The latter part, which lasts from 0.35 to 0.5, is disorganized.

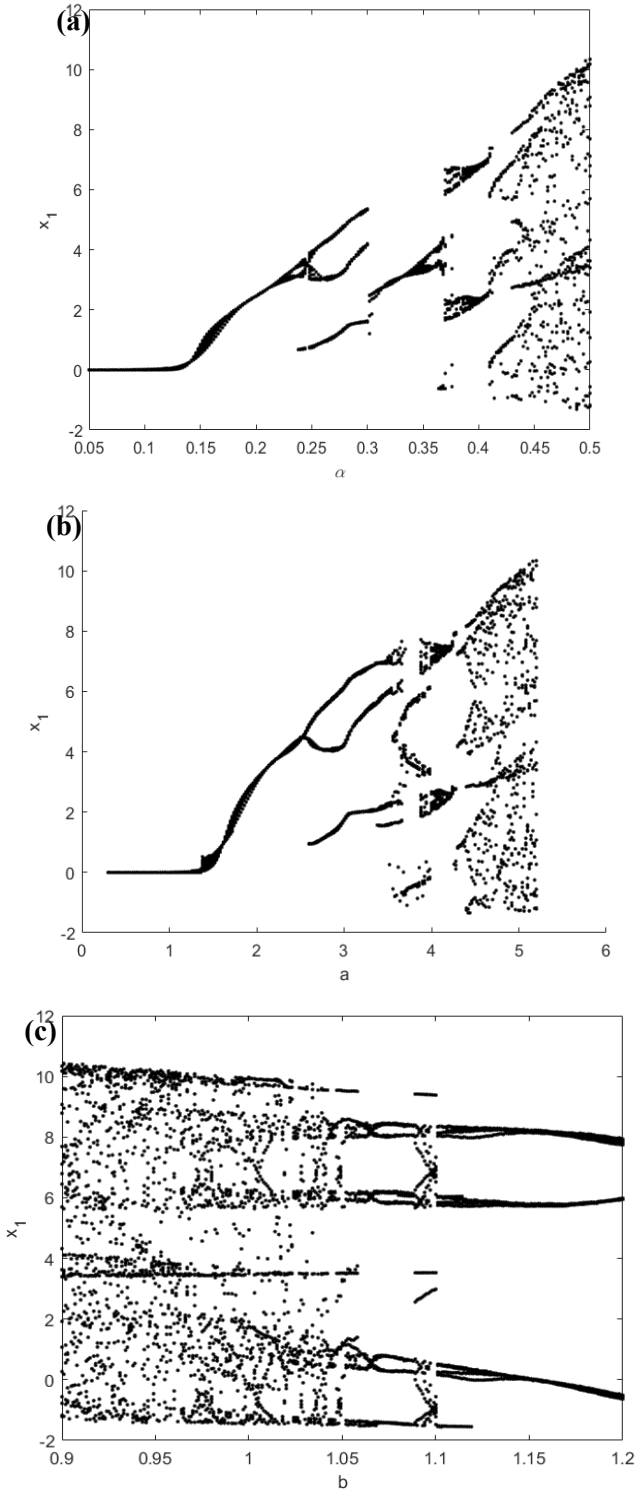

Fig. 16: The relationship between the voltages in the first capacitor and the control parameter (a) α , (b) a , (c) b.

By calculating the bifurcation values of the coefficient, a using the voltages within the first capacitor in Fig. (16(b)) at β = 0.1, α = 0.5, and b = 0.9, we can observe that the values are nearly identical to those in Fig. (16(a)) with the

difference in a value. The stability zone, it turns out, does not begin at zero. A distinct region appears after it hits 1.7, at which point we observe that the amplitude has grown while keeping the periodicity. There is a Periodic triad of 2.5 to 3.5. starting with the chaos zone at 3.5 to 5.2.

Regarding the bifurcation of b, we observe that it seems chaotic, ranging from 0.9 to 1.125, for the values $\alpha = 0.5$, $\beta = 0.1$, and $a = 5.2$ in Figure (16 (c)). It culminates in a periodic triplet of 1. 15 roughly to 1.2 and is dynamically rich.

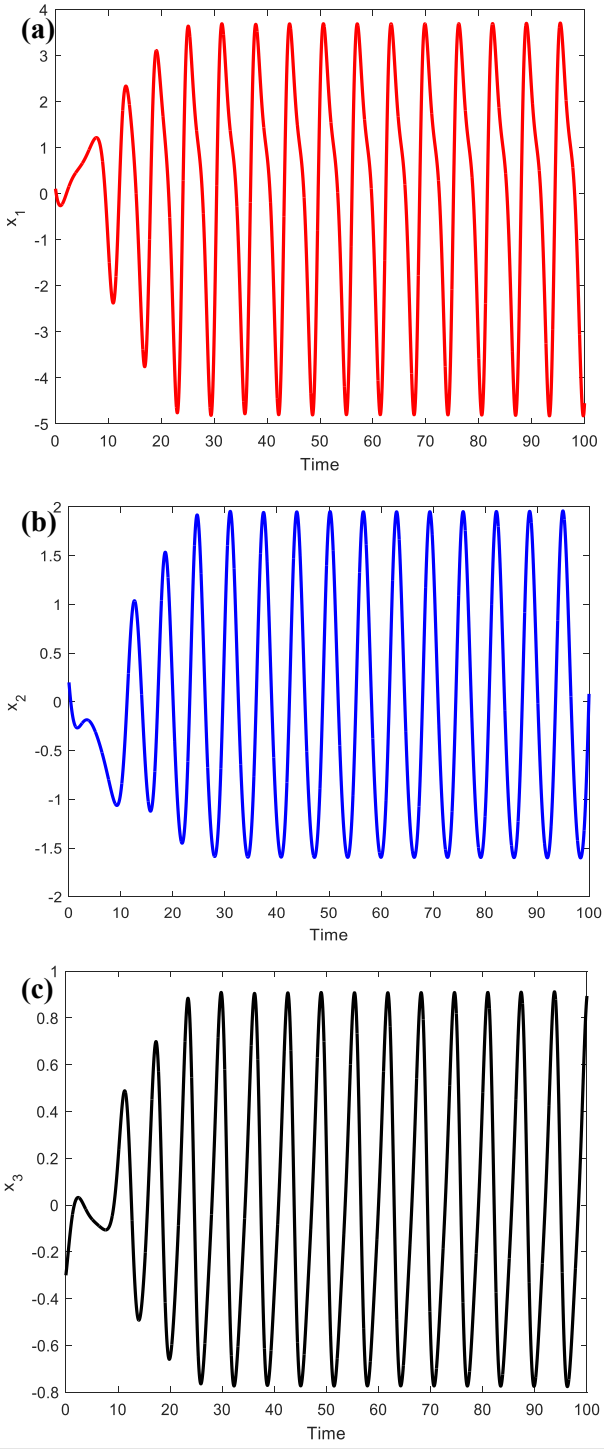

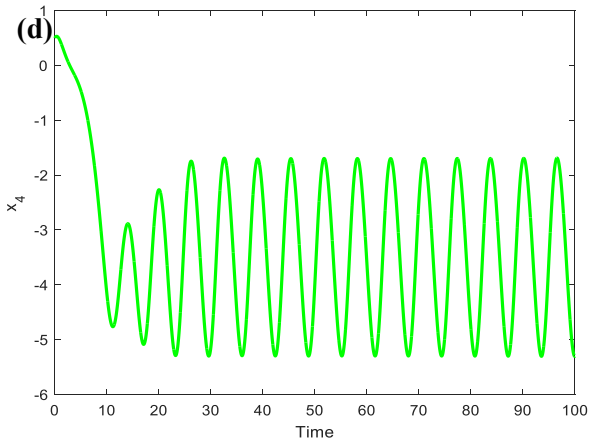

Fig. 17: Time series for Fig.(2.19 (b))when a=2.2.

The voltage within the first capacitor in Fig. (17(a)) and the voltage across the second capacitor in Fig.(17(b)) can be seen when looking at the time series in Fig. (16(b)) with values $\alpha = 0.5$, $\beta = 0.1$, $a = 2.2$, and $b = 0.9$. There is a periodic and stable state present in the voltage across the memristor (Fig. 17(d)) and the current flowing through the inductor Fig. (17(c)). The amplitude of the negative area in Fig. (17(d)) reduced dramatically because the negative component of the memristor formula was bigger than the positive portion; yet it continued to demonstrate periodic and stable behavior until the end of the series.

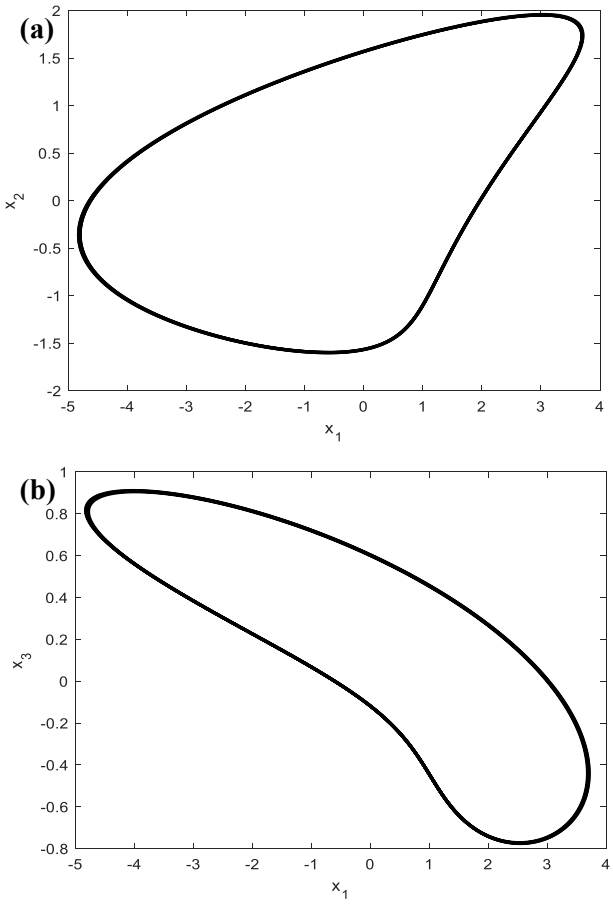

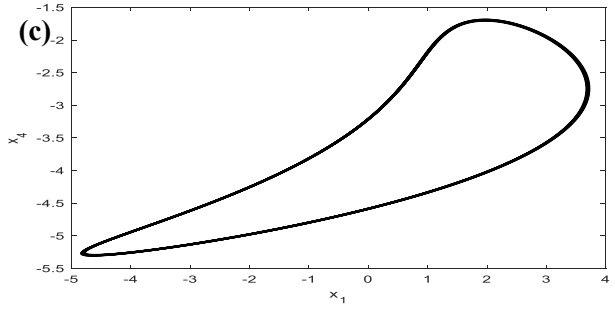

Fig. 18: Periodic diagrams of charge-controlled memristor based on Colpitts circuit between (a) x1-x2, (b) x1-x3, (c) x1-x4.

Although it is not quite symmetrical, the periodic state diagram between the voltages of the first and second capacitors in Fig. 18(a)) is depicted in Fig. (18). In Fig. (18(b)), the voltage through the first capacitor and the current across the inductor are similar to this, but they are not symmetrical. The relationship between the voltages through the first capacitor and the voltages in the memristor in Fig. (18(c)) is comparable to the two forms that came before it in the case of periodicity. Nonetheless, the Colpitts circuit will not be symmetrical if the nonlinear resistance in Fig. (15(b)) is substituted for the memristor. Despite losing its symmetry, the Colpitts circuit remained periodic and stable.

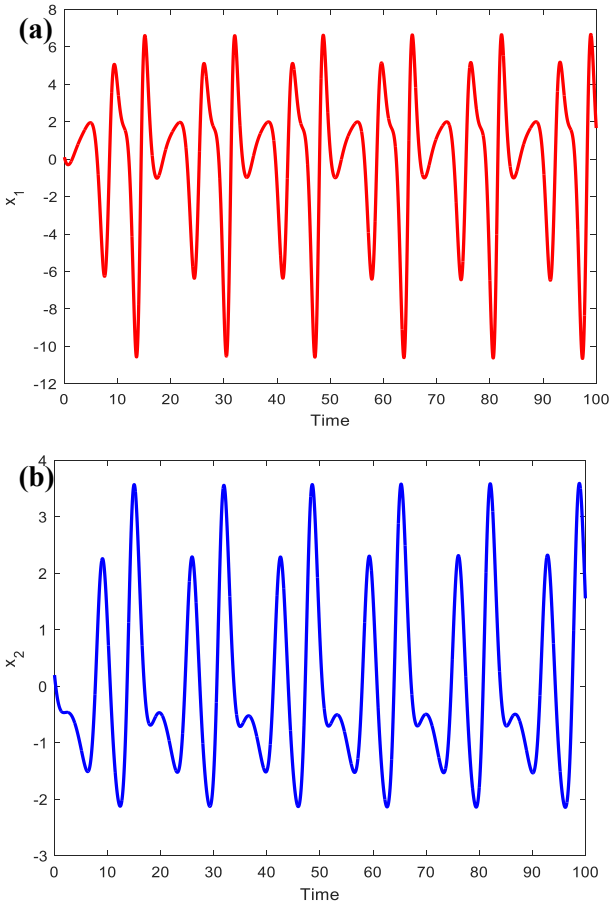

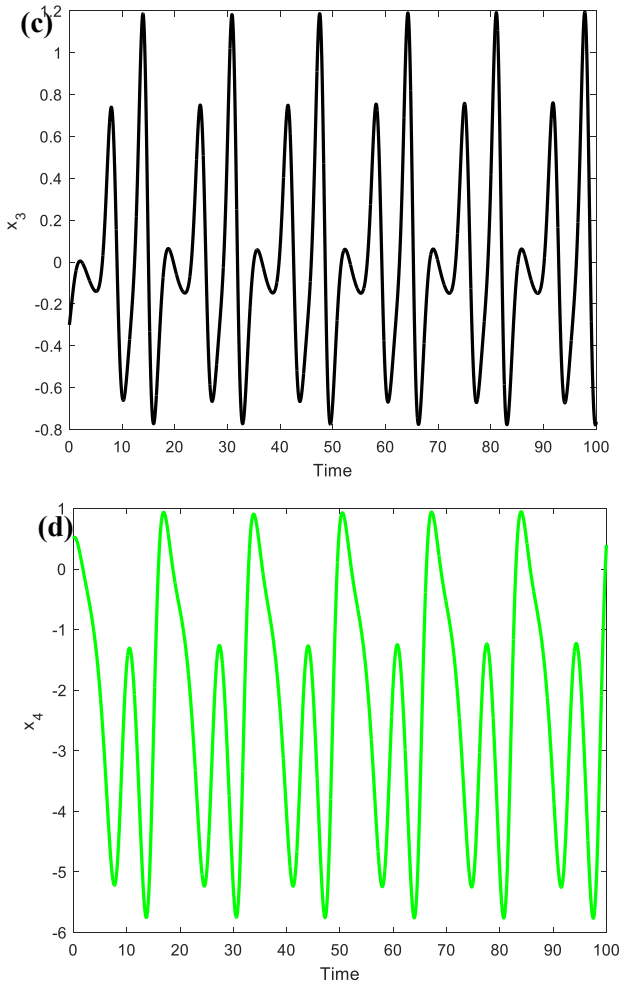

Fig. 19: Time series Fig.(19 (b))when a= 3.2

When we alter the value of (a = 3.2) in Fig. (19), we discover that the time series of the voltage changes in the first capacitor Fig. (19(a)) is in a double quasi-periodic condition; in other words, we observe repetition in both of them in Fig. (19(b)), but not stability. The voltage in the second capacitor likewise serves as a representation of the voltage's prior behavior. Although there is symmetry in terms of recurrence in the time series of the current through the inductor, we discover quasi-double periodicity Fig. (19(c)). As in the earlier representations, we locate it in the quasi-periodic binary state. Here, there is a pattern of conduct. The voltage within the memristor in Fig. (19(d)) repeats the same process.

The plots of the charge-controlled memristor in a Colpitts circuit to Fig. (19) to a depiction of the voltages in the first and second capacitors in Fig. (20(a)) exhibit a twofold periodic irregularity when we raise the value of (a = 3.2). On the other hand, Fig. (20(b)) shows about half of a triple cycle when we look at the voltage of the first capacitor and the current flowing through the inductor. As previously, though, we observe that it is not symmetric. Since the negative component of the voltage is more periodic than the

negative part, this discovery is also evident by viewing the voltages between the first capacitor and the memristor in Fig. (20(c)) as double quasi-periodic, albeit without symmetry.

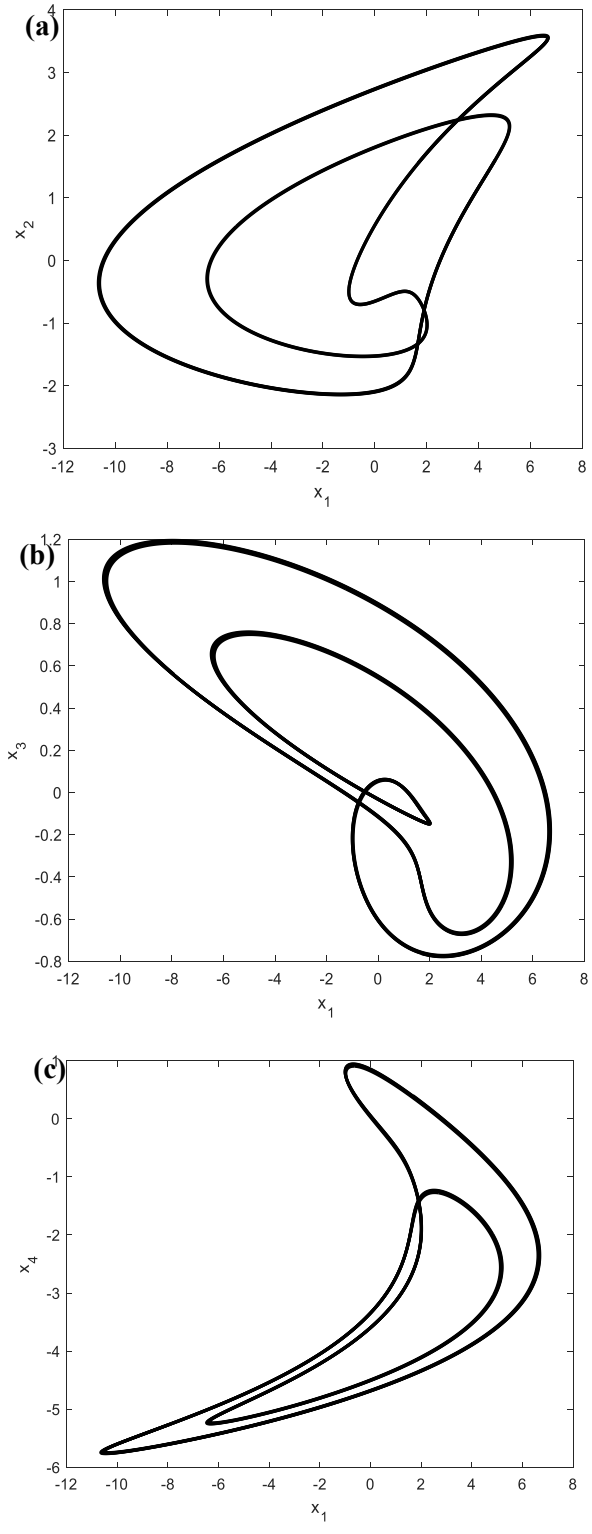

Fig. 20: Quasi-periodic double plots of the charge-controlled memristor in a Colpitts circuit (a) x1-x2; (b) x1-x3 (c) x1-x4.

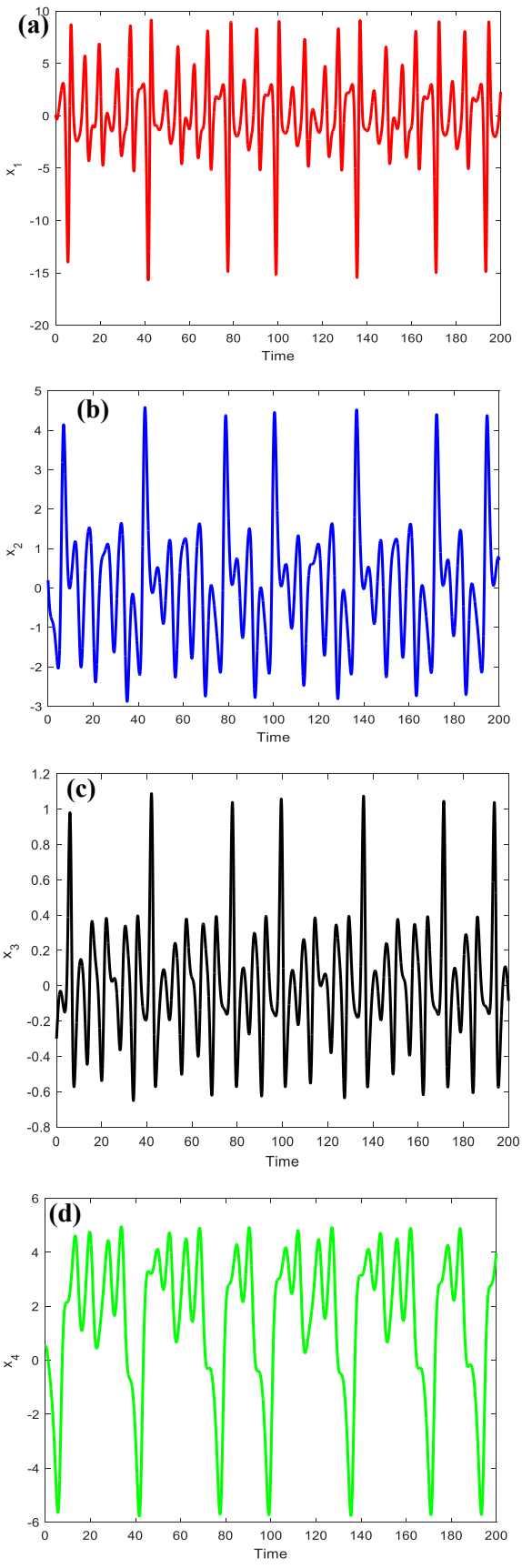

Fig. 21: Time series Fig.(19 (b)) when a=4.7.

We raised the value of (a = 4.7) in Fig. (21). The time series for each of the voltages in the first capacitor (Fig. 21(a)), second capacitor (Fig. 21(b)), memristor (Fig. 21(c)), and current flowing through the inductor (Fig. 21(d)) is found in Figure (19). These voltages produce quasi-periodic multiplicity, which repeats semi-regularly but is strewn with asymmetry in frequency.

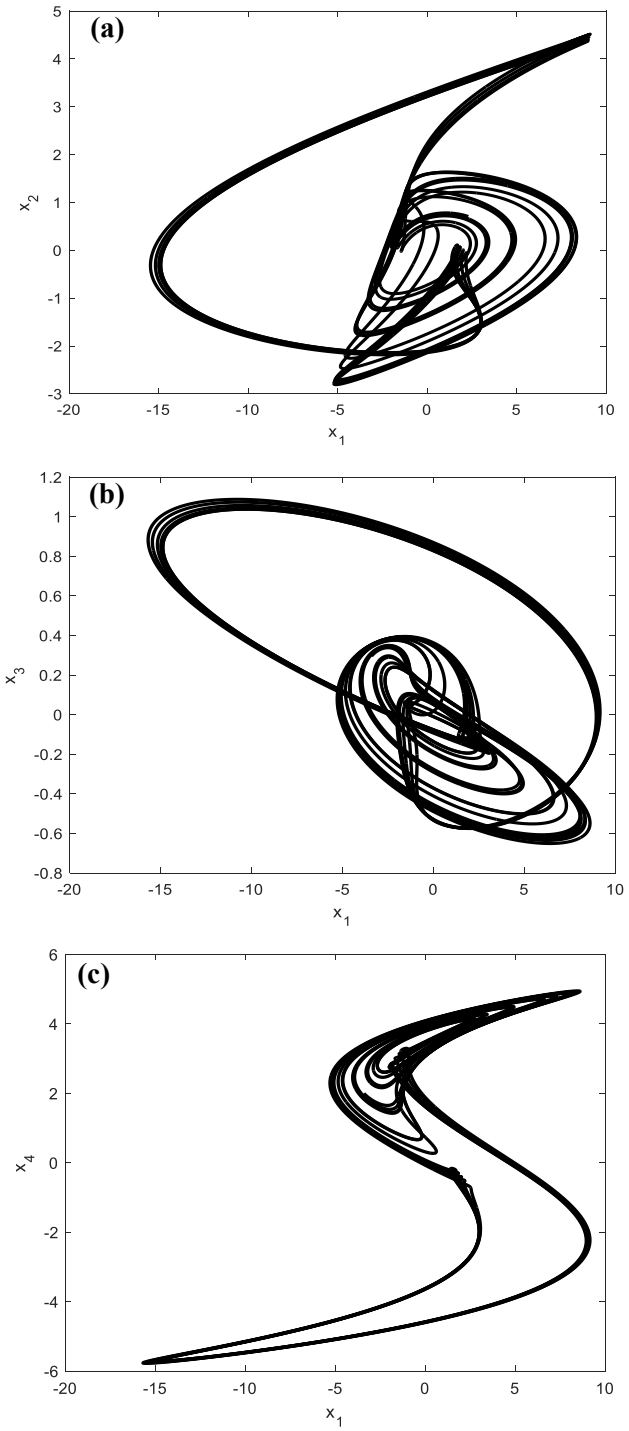

Fig. 22: The chaotic attractor is on the right side in (a) x_1-x_2; (b) x_1-x_3 (c) x_1-x_4.

Fig. (22(a)) displays a chaotic attraction. A peculiar, hyper-chaotic attractor was discovered by examining the voltages in the first and second capacitors, which indicates that the asymmetry and symmetry were obviously visible. Concerning Fig. (22(b)), we notice that he also discovered an absence of symmetry across the voltages in the first capacitor and the current flowing through the inductor. Additionally, he discovered an odd or too chaotic attractor. On the right side is where we also locate it. Fig. 22(c)) voltage range illustrates this. initial resistor and capacitor.

The increase in the value of (a) is what causes the asymmetrical and regular repeating of periodicity; that is, the higher the value of (a), the more asymmetric and peculiar attractors, such as hyper-chaotic attractors, develop.

4 Conclusion

We discovered that over the past few years, a large number of researchers have been interested in memristors and their applications in a variety of sectors, such as computers and integrated circuits. We also discover that memristors are being studied in numerous experiments and mathematical models with an emphasis on their dynamic behavior in memristor circuits. Several memory circuits with chaotic oscillations were shown in this work.

We discover that over the past few years, a large number of researchers have been interested in memristors and its applications in a variety of sectors, such as computers and integrated circuits. We also discover that memristors are being studied in numerous experiments and mathematical models with an emphasis on their dynamic behavior in memristor circuits. Several memory circuits with chaotic oscillations were shown in this work. Three circuits—Muthuswamy-chua, Chua, and Colpitts—will also be our main emphasis. We look at Muthuswamy, the most basic circuit, which consists of a capacitor and an inductor. Periodic attractions and chaos arise. Next, we take a look at the Chua circuit and change the Chua diode in favor of the memristor.

We find the chaotic and multiconjugate attractors, and then we find the Colpitts circuit, where the memory formula is used instead of the exponential formula. This produces a complicated profile that depends on several factors (a, b, d, c, α, and β), much like the prior two circuits did. Our findings indicate that chaotic behavior must alter as these parameters rise or fall, even though there are several stable states. We discover that increasing D led to more stable behavior in the Showa circuit, whereas increasing b led to more stable behavior in Muthuswamy. Instability results from rising or falling coefficients, much like in Colpitts. outcome of incorporating a memristor into an electrical circuit.

Acknowledgments: Support for this effort is provided by the Nasiriya Nanotechnology Research Laboratory (NNRL)

at the University of Thi-Qar, Iraq's Science College.

Compliance with ethical standards

Conflicts of interest: The writers have declared that they have no conflicts of interest.

Author contributions: All the authors contributed equally to this work. This work was made possible by the equal contributions of all authors.

Data Availability Statement. Data have been examined and incorporated in this publication. Detailed data could be supplied with the corresponding author upon a reasonable re This manuscript contains the results of data analysis. Upon reasonable request, detailed data could be given with the corresponding author.

References

[1] L. Chua, ‘‘Memristor-the missing circuit element’’, *IEEE Transactions on circuit theory*. 18(5),507–519(1971).

[2] R. S. Williams, ‘How we found the missing memristor’, *IEEE Spectr*, 45(12), 28–35(2008).

[3] A.C. Torrezan, J. P. Strachan, G. Medeiros-Ribeiro, and R. S. Williams, ‘Sub-nanosecond switching of a tantalum oxide memristor’, *Nanotechnology*. 22 (48) ,485203 (2011).

[4] S. Lv, J. Liu, and Z. Geng, ‘Application of Memristors in Hardware Security: A Current State-of-the-Art Technology’, *Advanced Intelligent Systems*. 3 (1), 2000127 (2021).

[5] H. Lin, C. Wang, Q. Hong, and Y. Sun, ‘‘A multi-stable memristor and its application in a neural network’’, *IEEE Transactions on Circuits and Systems II: Express Briefs*. 67(12), 3472–3476 (2020).

[6] B. Wang, F. C. Zou, and J. Cheng, ‘‘A memristor-based chaotic system and its application in image encryption’’, *Optik (Stuttg)*. 154 , 538–544(2018).

[7] Y. Tan and C. Wang, ‘‘A simple locally active memristor and its application in HR neurons’’, *Chaos: An Interdisciplinary Journal of Nonlinear Science*. 30 (5), (2020).

[8] M. T. Abuelmaatti and Z. J. Khalifa, ‘‘A new memristor emulator and its application in digital modulation’’, *Analog Integr Circuits Signal Process*. 80, 577–584 (2014).

[9] S. Shin, K. Kim, and S.-M. Kang, ‘‘Analysis of passive memristive devices array: Data-dependent statistical model and self-adaptable sense resistance for RRAMs’’, *Proceedings of the IEEE*. 100 (6), 2021–2032 (2011).

[10] F. A. S. Ferrari *et al.*, ‘‘Numerical simulations of the linear drift memristor model’’, *The European Physical Journal Plus*. 134 (3), 102 (2019).

[11] Y. N. Joglekar and S. J. Wolf, ‘‘The elusive memristor: properties of basic electrical circuits’’, *Eur J Phys*. 30 (4), 661 (2009).

[12] M. S. M. Al-Fayyadh, K. H. Ismael, and A. J. R. Al-Saady, ‘‘Study of insulin resistance, cortisol hormone and some biochemical parameters in Iraqi type 2 diabetic patients’’, *University of Thi-Qar Journal of Science*. 10 (2), 68–72 (2023).

[13] M. Shahsavari, ‘‘Memristor technology and applications: An overview’’, (2013).

[14] R. Mutlu and ertuğrul Karakulak, ‘‘A Simple Test For Memristors With High ROFF/RON Ratio’’. 2, 1–5 (2019).

[15] B. Muthuswamy and S. Banerjee, ‘‘*Introduction to Nonlinear Circuits and Networks’’*. (2018).

[16] R. Tetzlaff, ‘‘*Memristors and memristive systems’’*. Springer, (2013).

[17] X. Xie, L. Zou, S. Wen, Z. Zeng, and T. Huang, ‘‘A flux-controlled logarithmic memristor model and emulator’’, *Circuits Syst Signal Process*. 38 (4), 1452–1465 (2019).

[18] Y. N. Joglekar and S. J. Wolf, ‘‘The elusive memristor: properties of basic electrical circuits’’, *Eur J Phys*. 30 (4), 661 (2009) .

[19] F. A. S. Ferrari *et al.*, ‘‘Numerical simulations of the linear drift memristor model’’, *The European Physical Journal Plus*. 134 (3), 102 (2019).

[20] K. C. Iarosz *et al.*, “Chaotic dynamics in memristive circuits’’, *Revista Brasileira de Ensino de Física* . 45, e20230116 (2023).

[21] M. A. Rahma, E. A. Mohammed, and H. L. Saadon, ‘‘Linear and Nonlinear Optical Properties of Natural Dyes Freestanding Films and Application in Optical Limiting’’, *University of Thi-Qar Journal of Science*. 7(2), 139–143 (2020).

[22] M. A. Kadim *et al.*, ‘‘Nonlinear quantum dot light emitting diode dynamics and synchronization with Optoelectronic feedback’’, *University of Thi-Qar Journal of Science*, 10 (1), (2023).

[23] F. Corinto, M. Forti, and L. O. Chua, ‘‘*Nonlinear Circuits and Systems with Memristors: Nonlinear Dynamics and Analogue Computing via the Flux-Charge Analysis Method”*. Springer Nature, (2020).

[24] Z. Q. Chen, H. Tang, Z. L. Wang, Q. Zhang, and J. W. Han, ‘Design and circuit implementation for a novel charge-controlled chaotic memristor system’, *J. Appl. Anal. Comput* .5 (2), 251–261 (2015).

[25] B. Muthuswamy and L. O. Chua, ‘‘Simplest chaotic circuit’’, *International Journal of Bifurcation and Chaos*. 20 (05), 1567–1580 (2010).

[26] L. O. Chua and S. M. Kang, ‘‘Memristive devices and systems’’, *Proceedings of the IEEE*. 64 (2), 209–223 (1976).

[27] A. Sordi, ‘‘Chua’s oscillator: an introductory approach to chaos theory’’, *Revista Brasileira de Ensino de Física*. 43 , e20200437 (2020).

[28] T. Matsumoto, ‘‘A chaotic attractor from Chua’s circuit’’, *IEEE Trans Circuits Syst*. 31 (12) , 1055–1058 (1984).

[29] G. Zhong and F. Ayrom, ‘‘Experimental confirmation of chaos from Chua’s circuit’’, *International journal of circuit theory and applications* . 13 (1), 93–98 (1985).

[30] B. Muthuswamy, ‘‘Implementing memristor based chaotic circuits’’, *International Journal of Bifurcation and Chaos*. 20 (05) . 1335–1350 (2010).

[31] L. Teng, H. H. C. Iu, X. Wang, and X. Wang, ‘‘Chaotic behavior in fractional-order memristor-based simplest chaotic circuit using fourth degree polynomial’’, *Nonlinear Dyn*. 77, 231–241 (2014).

[32] K. Rajagopal, S. Kacar, Z. Wei, P. Duraisamy, T. Kifle, and A. Karthikeyan, ‘‘Dynamical investigation and chaotic associated behaviors of memristor Chua’s circuit with a non-ideal voltage-controlled memristor and its application to voice encryption’’, *AEU-International Journal of Electronics and Communications* . 107, 183–191 (2019).

[33] M. P. Kennedy, ‘‘Chaos in the Colpitts oscillator’’, *IEEE Transactions on circuits and systems I: Fundamental Theory and Applications* . 41 (11), 771–774 (1994).

[34] R. C. Bonetti *et al.*, ‘‘Super persistent transient in a master–slave configuration with Colpitts oscillators’’, *J Phys A Math Theor*. 47 (40), 405101 (2014).

[35] R. C. Bonetti And A. M. Batista, ‘‘Sincronização E Memórias Em Osciladores Colpitts Acoplados’’, (2014).

[36] G. M. Maggio, O. De Feo, and M. P. Kennedy, ‘‘Nonlinear analysis of the Colpitts oscillator and applications to design’’, *IEEE Transactions on Circuits and Systems I: Fundamental Theory and Applications*. 46 (9), 1118–1130 (1999).

[37] B. Bao, G. Zhou, J. Xu, and Z. Liu, ‘‘Multiscroll chaotic attractors from a modified colpitts oscillator model’’, *International Journal of Bifurcation and Chaos*. 20 (07), 2203–2211 (2010).

[38] Y. Wu, Q. Jin, W. Wang, and Y. Liu, ‘‘Asymmetrical passive intermodulation distortions of memristors with mathematical behavior models’’, *AIP Adv* . 6 (10), (2016).

[39] M. Karakayis and Y. Uyaroglu, ‘‘Synchronization Of Two Chaotic Behaviour Colpitts Oscillator’’, in *5th international Advanced Technologies Symposium*, (2009)